Computers and Geotechnics 42 (2012) 180–192

Contents lists available at SciVerse ScienceDirect

Computers and Geotechnics

journal homepage: www.elsevier.com/locate/compgeo

Cyclic lateral response of pile foundations in offshore platforms

Mohammad Mahdi Memarpour [a], Mehrdad Kimiaei [b,*], Mohsenali Shayanfar [a], Mostafa Khanzadi [a]

[a] Civil Engineering Department, Iran University of Science and Technology, Daneshgah St., Hengam Ave, Resalat Square, Narmak, Tehran 16846-13114, Iran
[b] Centre for Offshore Foundation Systems, The University of Western Australia, 35 Stirling Highway Crawley, WA 6009, Australia

ARTICLE INFO

Article history:
Received 7 July 2011
Received in revised form 24 October 2011
Accepted 13 December 2011
Available online 7 February 2012

Keywords:
Pile soil interaction
Offshore pile
BNWF model
Cyclic lateral load

ABSTRACT

Fixed offshore platforms supported by pile foundations are always subjected to lateral cyclic loads due to environmental conditions. In general, nonlinear pile–soil interaction is the most important source of nonlinear response of offshore platforms due to design environmental loads. Finite element models are high precision method in simulation of the pile soil interaction problems however these analyses are usually complex and computationally expensive. In contrast, Beam on Nonlinear Winkler Foundation (BNWF) models are versatile, efficient and can possess sufficient precision. In this paper a new robust and practical BNWF model is presented for lateral behaviour of pile foundations under cyclic lateral loads. This cyclic pile–soil interaction model is incorporated as a user element into a general finite element software (ABAQUS) and can be easily used for complicated nonlinear strength analysis of fixed platforms. Monotonic or cyclic loading, gap formation and development, drag force and different backbone curves recommended by American Petroleum Institute can be easily used in this BNWF model. This paper deals with the effects of cyclic pile soil interaction on lateral response of offshore piles. Different parts of this BNWF model are discussed and addressed in detail. The piles behaviour in an example fixed offshore platform are investigated under lateral cyclic and monotonic loadings.

1. Introduction

Pile-supported coastal and offshore structures in marine soil deposits are always subjected to large lateral loads. Usually, the critical lateral forces on piles used in coastal structures are due to berthing and mooring forces, whereas piles in offshore jacket platforms are subjected to cyclic lateral loads due to waves. Nonlinearity of the soil stress–strain behaviour and geometric nonlinearities, such as disjointing and sliding between pile and soil, are the most dominant factors on the pile response. Bea [1] performed a series of static push-over analyses on a fixed offshore platform, and showed that the first nine nonlinear events were concentrated in the foundation piles. Nonlinear pile–soil interaction (PSI) is one of the main parameters that can deeply affect the overall response of the supported structures.

Analyses of lateral pile response are categorized into three major distinct methods [2]:

- The limit analysis method in which the ultimate soil reaction is to be drawn from assumed ultimate displacement of pile [3];
- Finite element (FE) or boundary element (BE) continuum-based models which are computationally expensive and practically difficult;
- Linear and nonlinear Winkler spring methods based on p–y curves.

In direct numerical approaches, FE and BE methods are used for solving the pile–soil interaction problems in which the pile, surrounded by soil and the pile–soil interface are modelled all together in one integrated model. Yegian and Wright [4], Randolph [5], Trochanis et al. [6] and Bentley and El Naggar [7] used finite element method (FEM), whereas Kaynia and Kausel [8], and Sen et al. [9] implemented boundary element method (BEM) for the response analysis of piles. Millán and Domínguez [10] and Padrón et al. [11] used coupled finite and boundary element methods for dynamic response of pile supported structures under time harmonic excitations. Their presented models were able to take into account dynamic pile soil interaction in a rigorous manner. 3D finite element and boundary element techniques need excessive computational efforts for pile soil interaction analysis, and thus they are not frequently used in engineering practices. Modelling pile–soil separation, gap formation, gap developments and other interface nonlinearities, can prove to be complicated tasks in continuum-based models. In addition, 3D finite element or boundary element elastoplastic pile–soil interaction models cannot not be easily incorporated in commercially available structural

* Corresponding author. Tel.: +61 8 6488 1915; fax: +61 8 6488 1044.
E-mail addresses: memarpour@iust.ac.ir (M.M. Memarpour), kimiaei@civil.uwa.edu.au (M. Kimiaei), shayanfar@iust.ac.ir (M. Shayanfar), khanzadi@iust.ac.ir (M. Khanzadi).

0266-352X/$ - see front matter
doi:10.1016/j.compgeo.2011.12.007

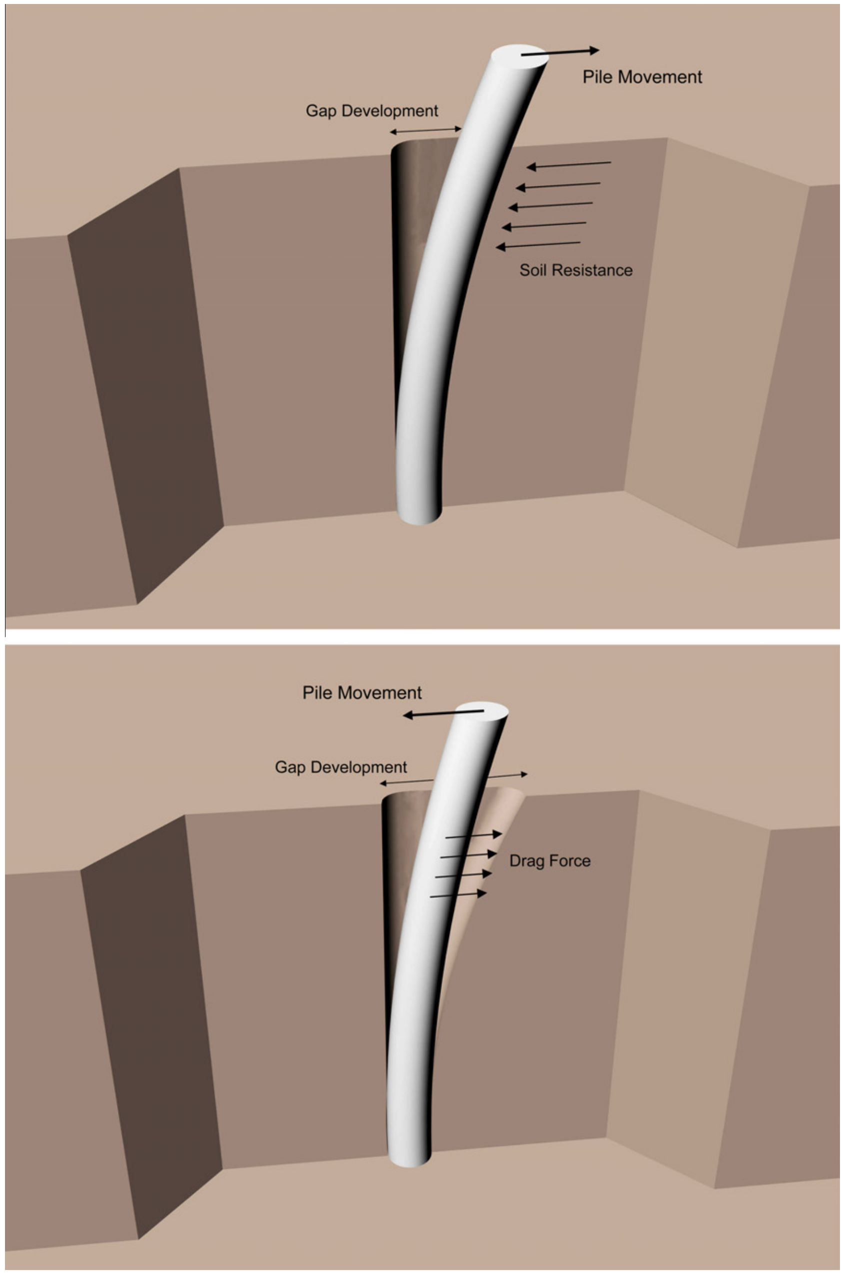

Fig. 1. Gap development and applied lateral forces on a pile during lateral deflections.

programs to compute the lateral response of complex offshore platforms as a whole.

Beam on Nonlinear Winkler Foundation (BNWF) models are computationally efficient and practically versatile, both for professional engineers in industrial design and in academia for research purposes. The method is of great use in comparison with continuum-based models and is continually the subject of further developments and modifications.

BNWF assumes that pile–soil interaction behaviour and force emerged in each soil layer are only related to soil displacement in the same depth and direction. Hence, it facilitates soil modelling by separated springs along the pile shaft. Matlock et al. [12], Makris and Gazetas [13], Nogami et al. [14] and El Nagger and Novak [15,16] proposed several models on the BNWF premise. Trochanis et al. [17] adopted the BNWF model with viscoplastic effect to study interaction behaviour in quasi-static and static conditions. Badoni and Makris [18] carried out several laboratory experiments

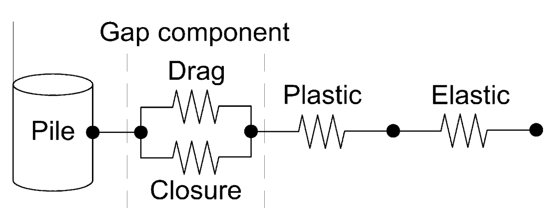

Fig. 2. BNWF spring components (Boulanger model [20]).

to verify results of Trochanis's model. Wang et al. [19] proposed several configurations of nonlinear springs and a parallel dashpot to investigate the damping field of BNWF soil–pile interaction models, mainly used in seismic studies. Boulanger et al. [20] proposed a configuration of parallel and series springs as well as a dashpot to incorporate nonlinear soil behaviour, gap formation in cohesive soils, drag force, and soil damping into BNWF models.

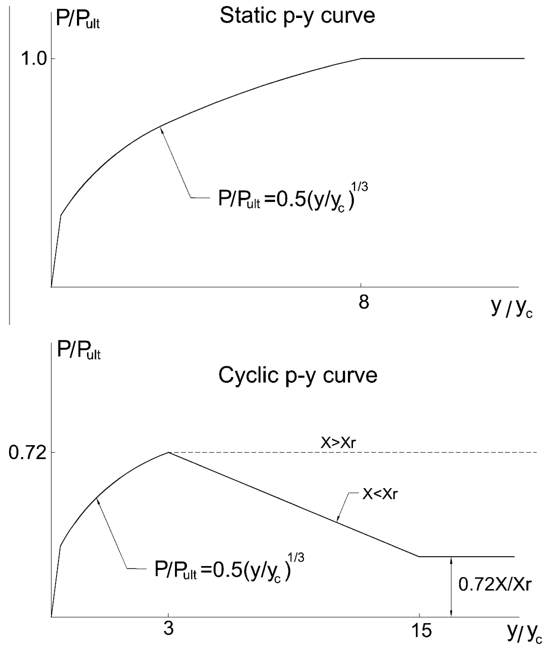

Fig. 3. Static and cyclic p–y curves as per API recommendations [31].

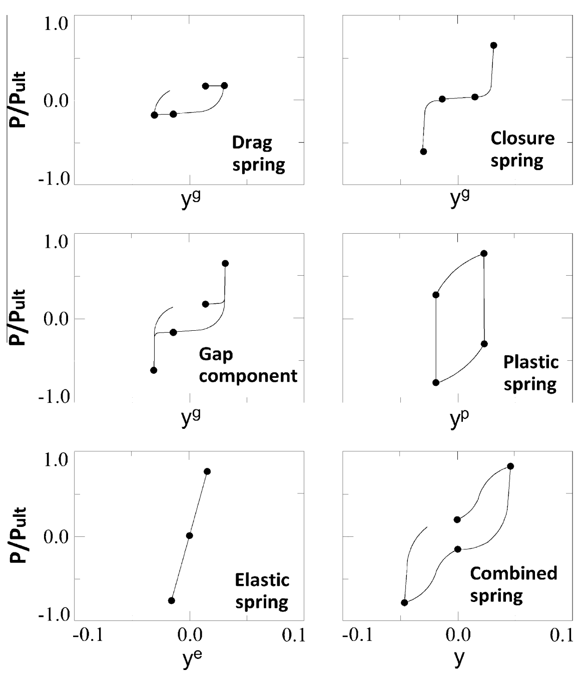

Fig. 4. Behaviour of CPSI components under cyclic loads using API static p–y curves.

Kimiaei et al. [21] proposed further modifications to integrate soil nonlinearity and gap formation into dynamic analysis of pile–soil interaction models. Gerolymos et al. [2] developed a numerical model and compared the results with laboratory experiments of fine non-cohesive soils. Wotherspoon et al. [22] used a simple BNWF model with allowance for gap developments for monotonic and cyclic response of piles in warm and frozen soil conditions. In this study using CPT and unconfined compression test data, bi-linear soil spring curves were developed to represent the soil hysteresis models. In general, assumptions associated with the BNWF models (particularly decoupling soil behaviour at different layers and in different directions) can potentially lead to deficiencies in the results. For example, as noted by Konuk and Fredj [23] and Fredj et al. [24], BNWF models for pipeline analysis are very sensitive soil spring coefficients and can produce conservative results. Care should be taken in using BNWF models for different problems and definition of the model components. Other approximate nonlinear methods with different philosophies have also been developed over the years such as Blum's method [25] and strain wedge method [26,27]. They can be of significant engineering interest for some cases. BNWF models are still the most popular models for pile soil interaction problems in engineering practices and can lead to reliable results.

BNWF models for pile–soil interaction problems require force–deflection (known as p–y, T–z) curves for the soil layers. These curves for soft clay [28], hard clay [29], and sand [30] soil layers are presented in the API [31] guidelines for analysis and design of offshore structures. In this study, a robust and practical BNWF model is proposed to integrate cyclic behaviour of piles under lateral cyclic loads. Commercially available finite element software ABAQUS [32] is used to develop this model. A comparative study is also performed on response of the pile foundation under cyclic and monotonic loading conditions along with a sensitivity analysis that is carried out over drag coefficient against dominant design variables.

2. Model description

Models used to analyse the structural response of piles under cyclic loads should allow for the variation of soil properties with depth, nonlinear soil behaviour and nonlinear behaviour of pile–soil interfaces. In general proper analysis of piles under lateral cyclic loads involves modelling of the piles, surrounding soils and the discontinuity conditions at the pile soil interfaces [21].

In this study, BNWF approach is used to investigate cyclic response of offshore piles under wave loads. General configuration of the suggested BNWF is based on the model presented by Boulanger et al. [20]. As shown in Fig. 1 resistance of the intact soil layers against the pile movements, separation between the pile and the soil (gap formation and development) and soil resistance when the pile moves in a previously developed gap area (drag force) are main components of this BNWF model. In this BNWF model the pile is modelled as series of discrete beam-column elements resting on a series of springs representing nonlinear behaviour of the soil.

Fig. 2 shows three main components of this BNWF model; elastic spring (p–y^e), plastic spring (p–y^p) and gap component (p–y^g) connected together in a series configuration. The gap component consists of a nonlinear closure spring (p^c–y^g) in parallel with a nonlinear drag spring (p^d–y^g) where:

$$p = p^d + p^c \tag{1}$$

$$y = y^e + y^p + y^g \tag{2}$$

Detail information about structural characteristics of these components can be found in Boulanger et al. [20]. The elastic spring has a constant stiffness determined from the soil characteristics and always acts linearly, while the plastic spring has two phases of behaviour. At the first phase when $-Cr.p_{ult} < p < Cr.p_{ult}$, the plastic spring acts rigidly. Cr is the ratio of p/p_{ult} when plastic yielding first occurs in virgin loading. The plastic spring behaviour in the second phase is formulated as follows:

$$p = p_{ult} - (p_{ult} - p_0)\left[\frac{c.y_{50}}{c.y_{50} + |y^p - y_0^p|}\right]^n \tag{3}$$

where p_{ult} is the ultimate resistance of the soil, $p_0 = p$ and $y_0^p = y^p$ both at the start of the current plastic loading cycle. Coefficients c and n control tangent module of the plastic spring and

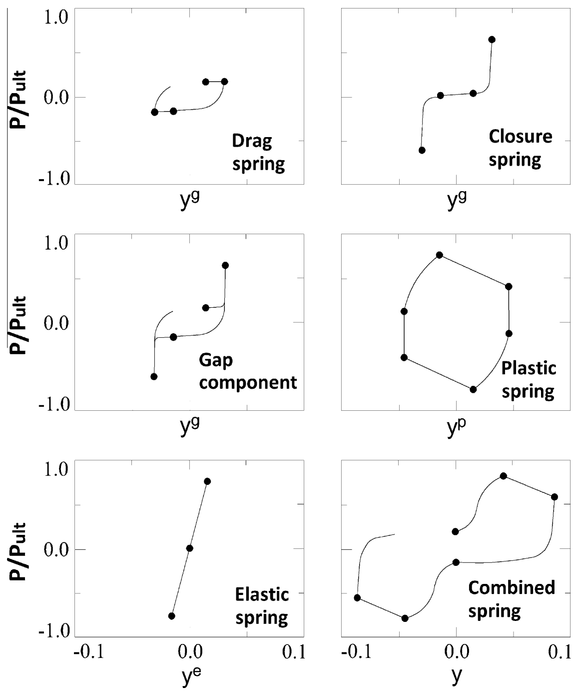

Fig. 5. Behaviour of CPSI components under cyclic loads using API cyclic *p*–*y* curves.

curve sharpness respectively. y_{50} is displacement at which 50% of p_{ult} is mobilized during static loading. p_{ult} shows ultimate lateral capacity of the soil layer and will be updated during each load step in the BNWF model. The nonlinear drag spring in gap component can be defined as follows:

$$p^d = C_d p_{ult} - (C_d p_{ult} - p_0^d)\left[\frac{y_{50}}{y_{50} + 2|y^g - y_0^g|}\right] \tag{4}$$

where C_d determines maximum drag force according to the ultimate resistance of the soil, $p_0^d = p^d$ and $y_0^g = y^g$ at the start of the current loading cycle. The drag spring emerges a constant force in the gap zone and when the gap closes, it is rendered inactive so that the elastic and the plastic springs activate. For continuous transition between active components (elastic/plastic vs. drag), a closure spring is provided in parallel configuration with the drag spring. In closure spring y_0^+ and y_0^-, defined in Eq. (5), act as a buffer to preserve the gap region from the previous cycle for positive and negative sides of the gap. The initial values of y_0^+ and y_0^- are set as $y_{50}/100$ and $-y_{50}/100$, respectively. Ultimately when y^g increases to the magnitude of the previous cycle, the gap actually closes analogously and the gap component will be inactive due to the drastic increase in its stiffness and force.

$$p^c = 1.8 p_{ult}\left[\frac{y_{50}}{y_{50} + 50(y_0^+ - y^g)} - \frac{y_{50}}{y_{50} - 50(y_0^- - y^g)}\right] \tag{5}$$

The flexibility of the above equations can be used to approximate different *p*–*y* backbone curves. Matlock's [12] recommended backbone for soft clay is closely approximated using $c = 10$, $n = 5$ and $Cr = 0.35$ for static backbone curve and $c = 4$, $n = 5$ and $Cr = 0.35$ for cyclic backbone curve [33]. API's [31] recommended backbone for drained sand is closely approximated using $c = 0.5$, $n = 2$, and $Cr = 0.2$ for static and cyclic curves [28].

The BNWF model developed in this study, called Cyclic Pile Soil Interaction (CPSI), is capable of modelling hysteretic behaviour of soil layers according to the static or cyclic *p*–*y* backbone curves presented in the API code [31]. Fig. 3 shows API *p*–*y* static and cyclic backbone curves for soft clay layers. CPSI model can capture lateral behaviour of piles under monotonic and cyclic loads, gap phenomenon and drag force on the piles as well. Soil type (clay or sand), P_{ult}, y_{50}, C_d and X/X_r (depth ratio for reduced resistance zone according to API) are main input data for soil layers in CPSI. Typical force deflection behaviour for the main components of the CPSI model using API static and cyclic *p*–*y* curves are shown in Figs. 4 and 5 respectively.

CPSI model is implemented as a robust single node user element in a commercial finite element software ABAQUS. A brief flow chart for CPSI user element is illustrated in Fig. 6. The CPSI model is mainly developed for ultimate strength analysis of pile supported platforms under extreme wave loads. CPSI user can easily switch between monotonic loading (gradual load increase from zero to maximum with no gap development) and cyclic loading (time varying loads). Cyclic loading leads to gap formation and gap development in cohesive soil layers. The API static or cyclic *p*–*y* curves can be used as backbone curves for each loading condition. The user can also change the drag force amplitude to the desired level. To employ CPSI in an ABAQUS simulation, pile and surrounding soil are discretized into finite number of layers. Pile segments will be modelled by two-node standard beam-column elements. CPSI user element, showing pile–soil interaction behaviour, will be used for each soil sub layer and its stiffness will be updated in each load step according to the resultant soil deformation. A specific subroutine has been implemented in CPSI for better convergence of the numerical solutions. In this subroutine, large pile displacements associated with each load increment will be divided into some smaller displacements internally and then soil properties will be updated in each of these sub increments. In this way less unbalanced forces are obtained at the end of each increment

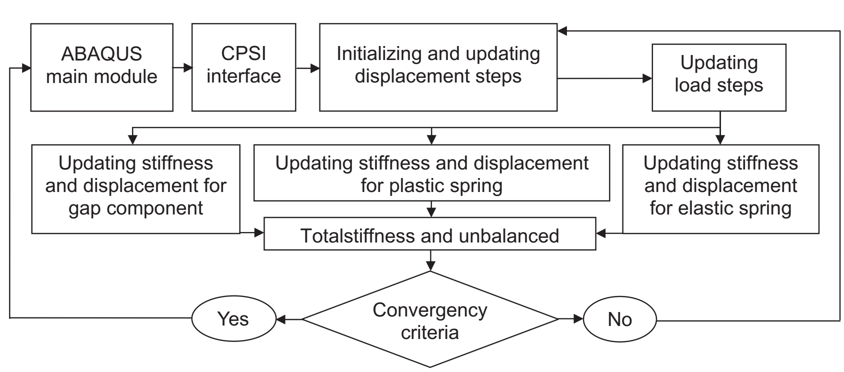

Fig. 6. Brief flow chart of CPSI user element in ABAQUS.

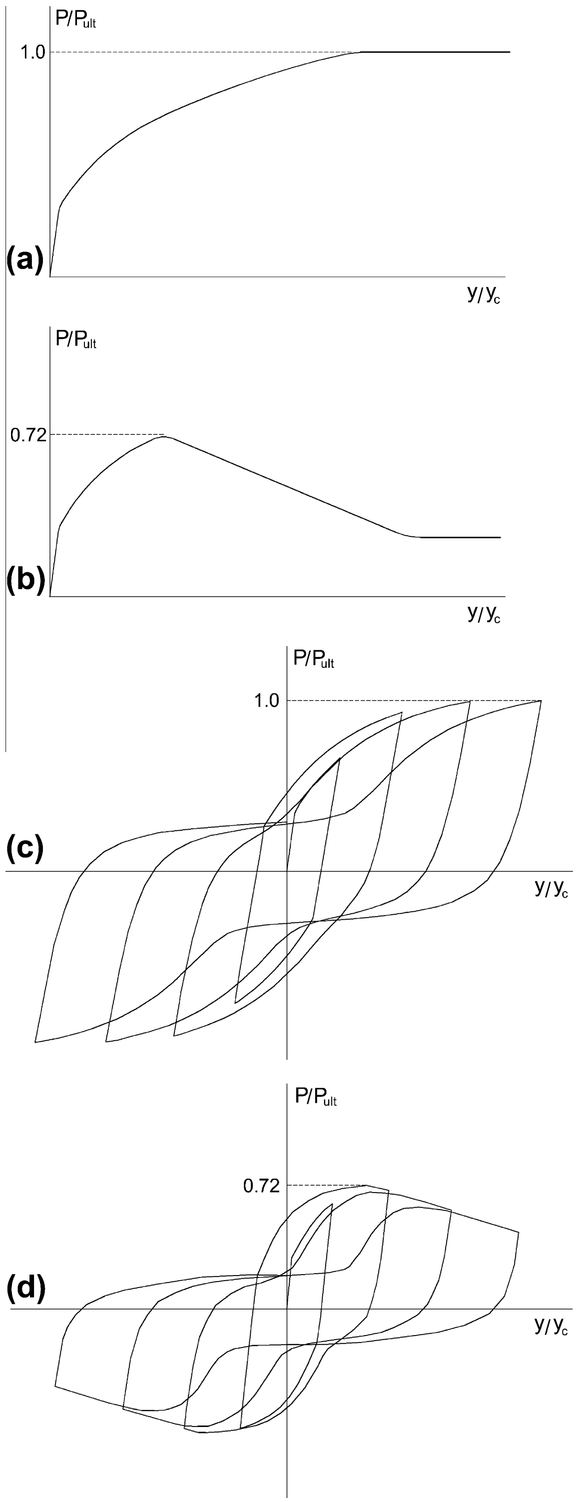

Fig. 7. Typical behaviour of CPSI elements (a) under monotonic loads using static p–y curves, (b) under monotonic loads using cyclic p–y curves, (c) under cyclic loads using static p–y curves, and (d) under cyclic loads using cyclic p–y curves.

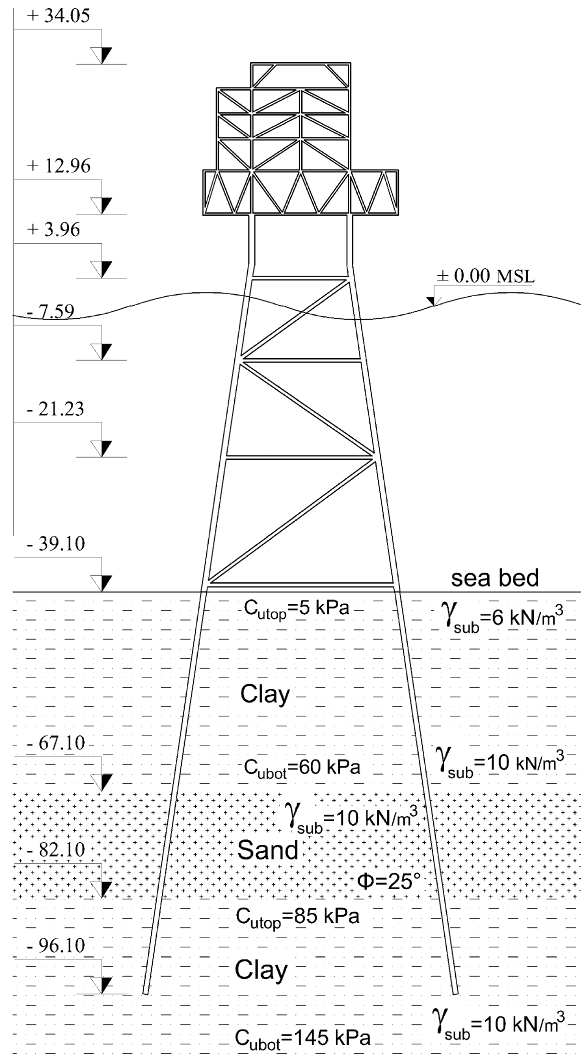

Fig. 8. General view of the jacket frame.

and hence it will help the CPSI code to capture strong pile–soil nonlinearities in a more stabilized manner. Ultimately, soil stiffness computed by CPSI will be inserted into the global stiffness matrix of the whole system in ABAQUS for the running simulation. More detail information about the numerical algorithm for the CPSI elements and verification of the results can be found in Memarpour et al. [33]. Fig. 7 displays typical behaviour of CPSI elements under monotonic and cyclic loads using API static or cyclic curves [34].

Concepts of the BNWF model used in the CPSI code have already been validated against centrifuge test results by Boulanger et al. [20] for single piles under dynamic motions. This BNWF model has also been implemented in OpenSees program [35] and its numerical results for single piles under lateral loads have been verified with the experimental results by Wallace et al. [36]. Memarpour et al. [33] showed very good agreement between CPSI and OpenSees results for a single pile under cyclic loads.

3. Case study

3.1. Example platform

Fig. 8 shows a 2D frame of an example pile supported jacket type platform used in this study. This platform is a four-legged jacket with single diagonal bracing at each bay on the vertical frames and one through leg pile at each corner. The jacket dimensions in the horizontal plane at the top (deck-leg work point) and bottom (seabed level) are 13.7 m and 26.5 m respectively. The mean water depth is 39.1 m, the jacket total height is 44.0 m and

Table 1
Dimensions of the pile segments below seabed.

Element size	Depth below sea bed
0.25 m	0.0 to −5 m
0.50 m	−5 to −15 m
1.00 m	−15 to −35 m
2.00 m	−35 to −57 m

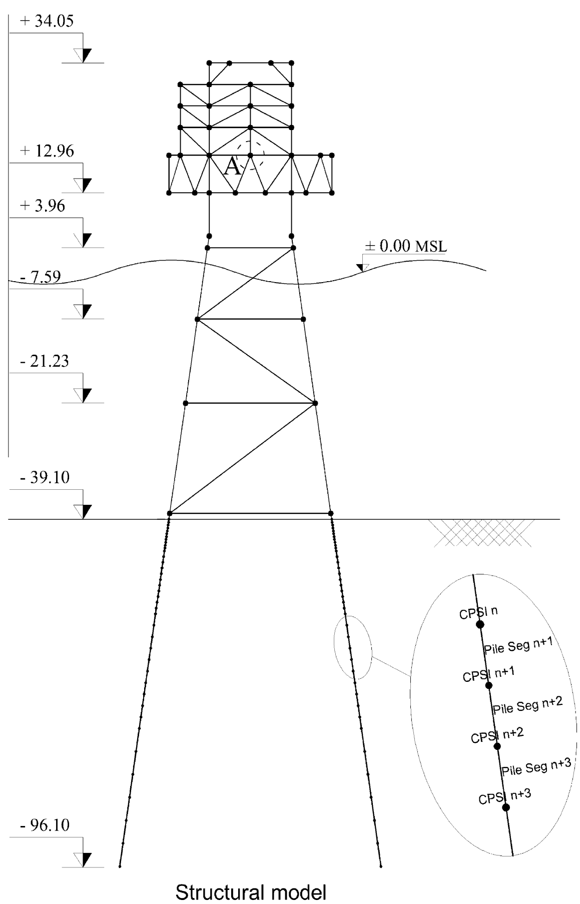

Fig. 9. Structural model of the jacket frame.

the piles are driven to total depth of 57.0 m below seabed. The outside diameters and wall thickness of the piles below seabed level are 32″ (81.28 cm) and 1.25″ (3.18 cm) respectively. The topside as a whole is a four-storey space frame on top of a one-storey deck. The soil profile consists of three horizontal soil layers of clay, sand and clay from top to bottom with respective depth of 28.0 m, 15.0 m and 14.0 m. Soil data is presented in Fig. 8.

3.2. Applied loads

Dead and live loads were applied as distributed loads on the platform members. Total applied dead and live loads on this 2D frame were 7800 kN and 4400 kN respectively. Environmental loads (including of wave, current and wind) were also applied on this frame. Wind loads (235 kN in total) and wave loads (total 1400 kN) were applied as point loads on topside and jacket main nodes. Initially dead, live and wind loads were applied as monotonic loads on the platform and then wave loads were applied in two different scenarios as monotonic and cyclic loads. In monotonic loading, wave loads were increased gradually from zero up to their design level, while in cyclic loading, a harmonic sinusoidal time-history function was used to represent the wave loading on the platform.

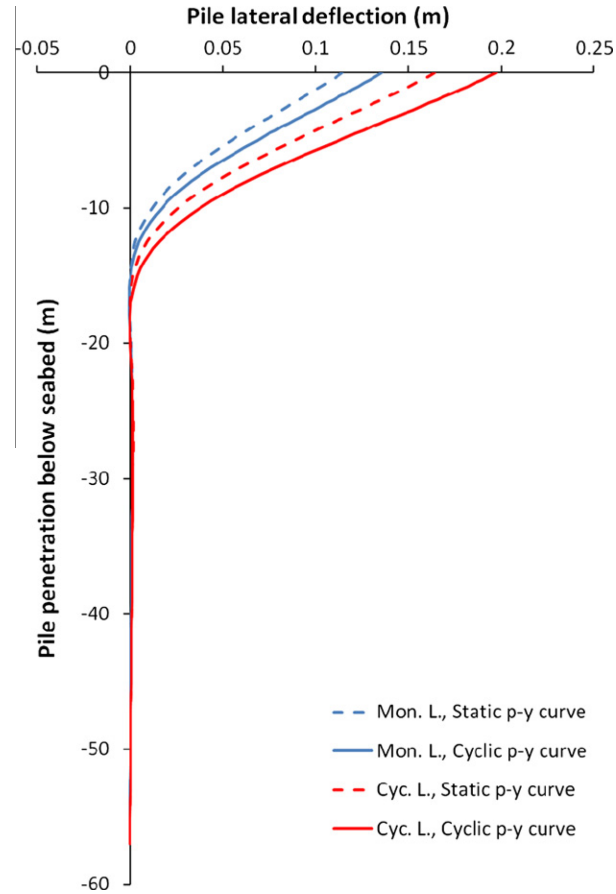

Fig. 10. Lateral deflection along the pile shaft in monotonic and cyclic loadings.

3.3. Structural model

ABAQUS was used for all structural analysis in this study. Standard two-node beam-column elements from ABAQUS element library in the elastic limits were used for modelling of the topside, jacket and pile members. Neither shear deflections nor other plastic features of the elements were used in this model. This model consisted of 210 elements in total for structural modelling of the jacket and the topside members.

Piles and surrounding soil layers were divided into 71 sub layers in total and CPSI user elements, showing pile–soil interaction, were implemented at all pile nodes below the seabed. 190 pile elements and 142 CPSI elements in total were used in this model. Pile segments in upper soil layers are usually subjected to higher lateral deflections and hence, in order to maintain accuracy and efficiency in numerical simulations, smaller pile segments should be used in the top soil layers. Table 1 shows the dimensions of the pile segments below seabed and Fig. 9 reveals the structural model of this jacket frame.

4. Discussion and numerical results

Pile deformations, internal forces and lateral displacement of the platform are considered here as the main parameters to inves-

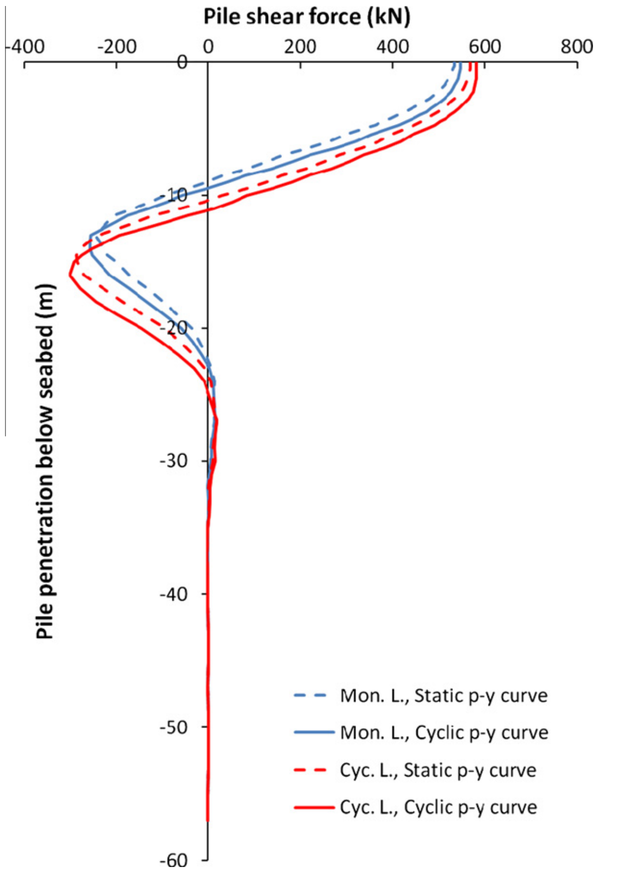

Fig. 11. Shear force distribution along the pile shaft in monotonic and cyclic loadings.

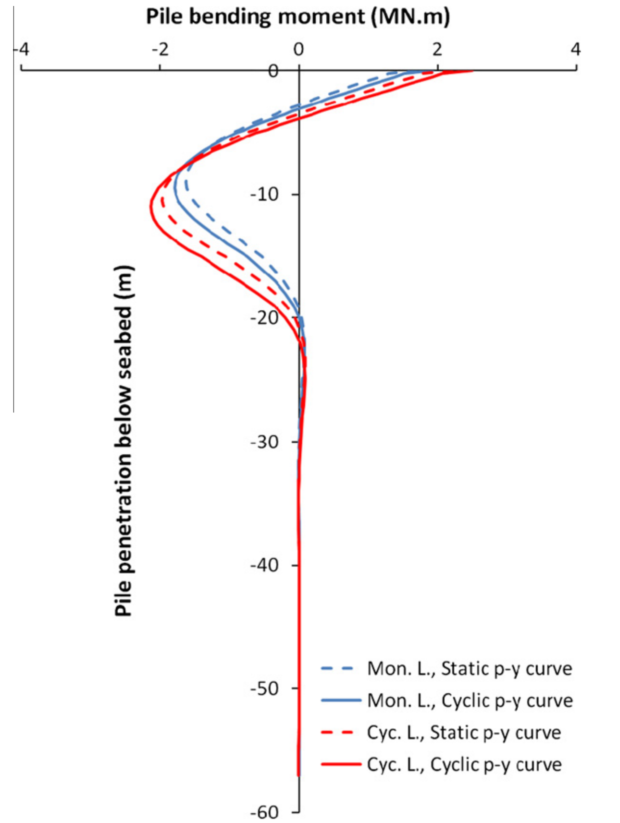

Fig. 12. Bending moment distribution along the pile shaft in monotonic and cyclic loadings.

tigate the sensitivity of the platform responses to different pile–soil interaction models. The main objective of the numerical simulations carried out in this study is to compare the overall response of the example platform under cyclic and monotonic loading. Gap development and drag force effects are also studied.

In the first step of this study, a comparison is made between the platform responses under monotonic and cyclic lateral loads. Figs. 10–12 show pile deflection, shear force and bending moment distributions along the pile shaft under monotonic and cyclic lateral loadings (after 10th cycle of the loading) respectively. It is seen that always using the cyclic p–y curves leads to the higher response of the pile than those of the static p–y curves, due to the soil strength reductions in API cyclic p–y curves compared with static p–y curves. It is also observed that all the pile responses under cyclic loads are higher than the pile responses under monotonic loads. In cyclic loading a gap is formed behind the pile (in cohesive soil layers) during the first loading cycle and then it will be developed gradually in subsequent loading cycles. This means that only the drag force (which is less than the soil resistance in the intact zones) can be taken by the soil layers when the pile starts moving in the previously created gap zones. In other words, because of the gap formation and gap developments in the cohesive soil layers, less load can be taken by top soil layers and therefore more load should be taken by the pile segments in those areas. It increases pile internal forces (bending moments and share forces) as well as pile lateral deflections. It will also move the critical sections of the pile (section with maximum bending moment or shear force along the pile shaft) to the lower soil layers.

Table 2
Result of pile maximum responses under monotonic and cyclic loads.

Pile response	Loading	Static p–y curve	Cyclic p–y curve	Difference (%)
Deflection (m)	Monotonic	0.114	0.136	19.3
	Cyclic	0.166	0.200	20.5
	Cyclic diff. (%)	45.6	47.1	–
Shear force (kN)	Monotonic	245	258	5.3
	Cyclic	287	302	5.2
	Cyclic diff. (%)	17.1	17.1	–
Bending moment (MN m)	Monotonic	1.63	1.79	9.8
	Cyclic	1.98	2.15	8.6
	Cyclic diff. (%)	21.5	20.1	–

Piles design parameters (maximum deflections, maximum shear forces and maximum bending moments) under monotonic and cyclic loads are summarized in Table 2. It shows that the increases in the pile deflections under cyclic loads are more crucial than other design parameters. It is also observed that the differences between the results for cyclic and monotonic loadings are greater than the differences between the results for static and cyclic backbone curves. It reveals that gap development phenomenon which is seen in cyclic loading model will influence the overall response of the pile more than soil strength degradation which is captured in cyclic p–y curves.

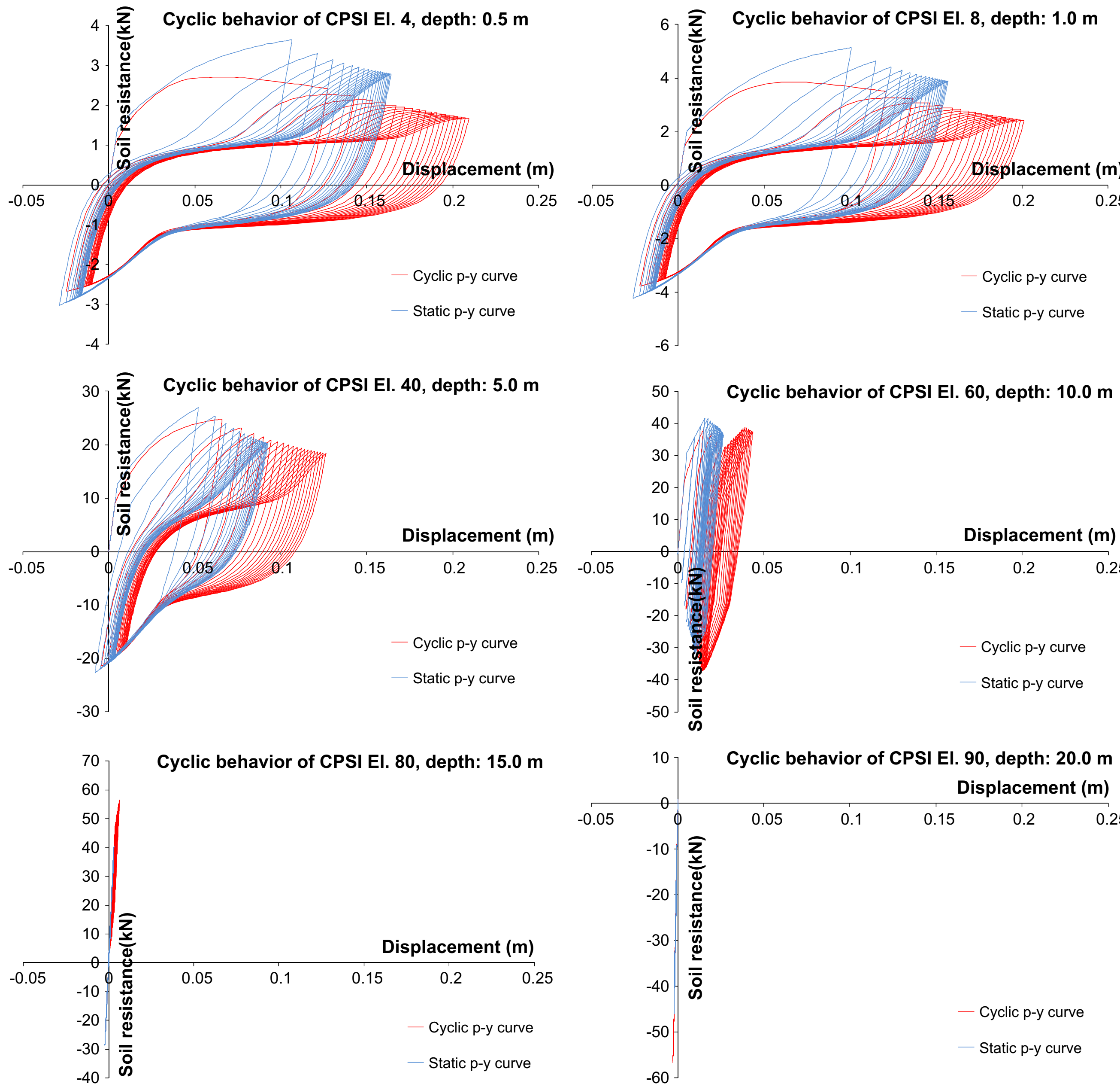

Fig. 13. Hysteretic soil reactions due to cyclic loads at different soil layers.

Hysteretic loops for soil reactions in different layers due to cyclic loads are shown in Fig. 13. Considerable differences between the static and cyclic *p–y* results for the soil reactions and the corresponding soil deformations can be seen in this figure. Top soil layers are more affected by cyclic backbone curves, mainly due to bigger gap developments in these areas. Cyclic displacements at each layer are larger than static results, because of soil strength reduction in cyclic *p–y* curves. General trend of the soil hysteretic loops in this figure for surface to deep soil layers are in reasonable agreement with the research results by others (e.g. Grabe et al. [37] and Wallace et al. [36]).

In order to investigate the pile behaviour during cyclic loading, time histories of the pile responses (deflections, shear forces and bending moments) at different depths are illustrated in Figs. 14–16. They all show that the maximum response of the pile increases gradually, and ultimately reaching a constant asymptotic value. In these figures it is seen that the rate of the pile response changes in the top soil layers is greater than the bottom layers. Pile responses using static *p–y* backbone curves reach a constant amplitude faster than the cyclic backbone curves. This is mainly due to the soil strength degradation and gap developments which are more severe in the top layers using cyclic *p–y* curve. During this process more loads will be transferred, cycle by cycle from top soil layers to the bottom soil layers.

In Fig. 14 it is observed that the pile deflection increases cycle by cycle until the 10th cycle, using static *p–y* curve, and then it continues with a constant amplitude. On the contrary, for the cyclic *p–y* curve where it reaches an almost constant amplitude in the 18th cycle. Shear forces and bending moments in Figs. 15 and 16 represent the same trend as seen for the pile deflection in Fig. 14. They show a quick rise in the pile internal forces over the first few cycles for both static and cyclic *p–y* backbone curves

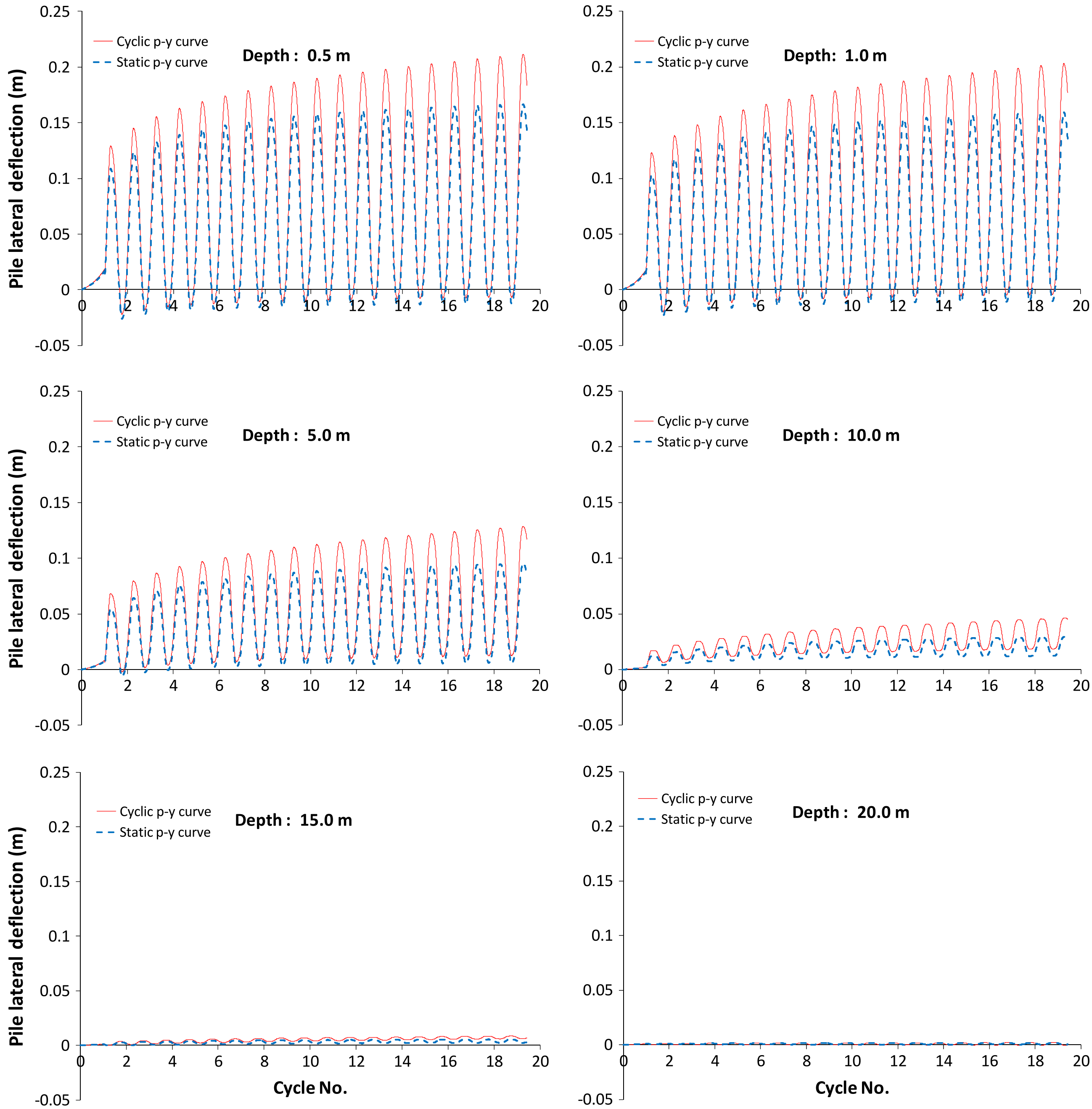

Fig. 14. Pile lateral deflections at different soil layers.

and then this rate decreases quickly in the following load cycles. The pile shear forces and bending moments reach constant amplitudes after the 10th and the 14th cycles for static p–y and cyclic p–y curves respectively. Moving from the surface to the deep soil layers, larger differences between shear forces and bending moments for static and cyclic p–y curves can be observed in Figs. 15 and 16.

From a pile design perspective, maximum internal forces and the location of the pile's critical section (where the maximum internal forces along the pile shaft are occurring) due to cyclic loading, as represented in Figs. 17 and 18, are important outcomes which should be studied. Fig. 17 shows an initial gradually increasing trend in both maximum shear forces and maximum bending moments. In Fig. 18, the critical section of the pile for shear forces and bending moments moves downward along the pile shaft during the first few cycles of the loading and then it reaches to a fixed position. Internal forces and the location of the critical sections are stabilized after few cycles. It is also seen that the pile responses (maximum amplitudes and critical location) using cyclic p–y backbone curves are always larger and also more sensitive to cyclic loads than static p–y curves.

All observations in Figs. 13–18 are due to gap formation and then gap developments (during cyclic loading) and soil strength reduction (as per cyclic p–y curves). Due to the gap development process more loads will be transferred cycle by cycle from top layers to the bottom soil layers and hence pile segments should be able to transfer those loads. After few cycles the whole system will reach a stable condition where the total loads to be taken by the tops soil layers (in the gap area) and the bottom soil layers (in

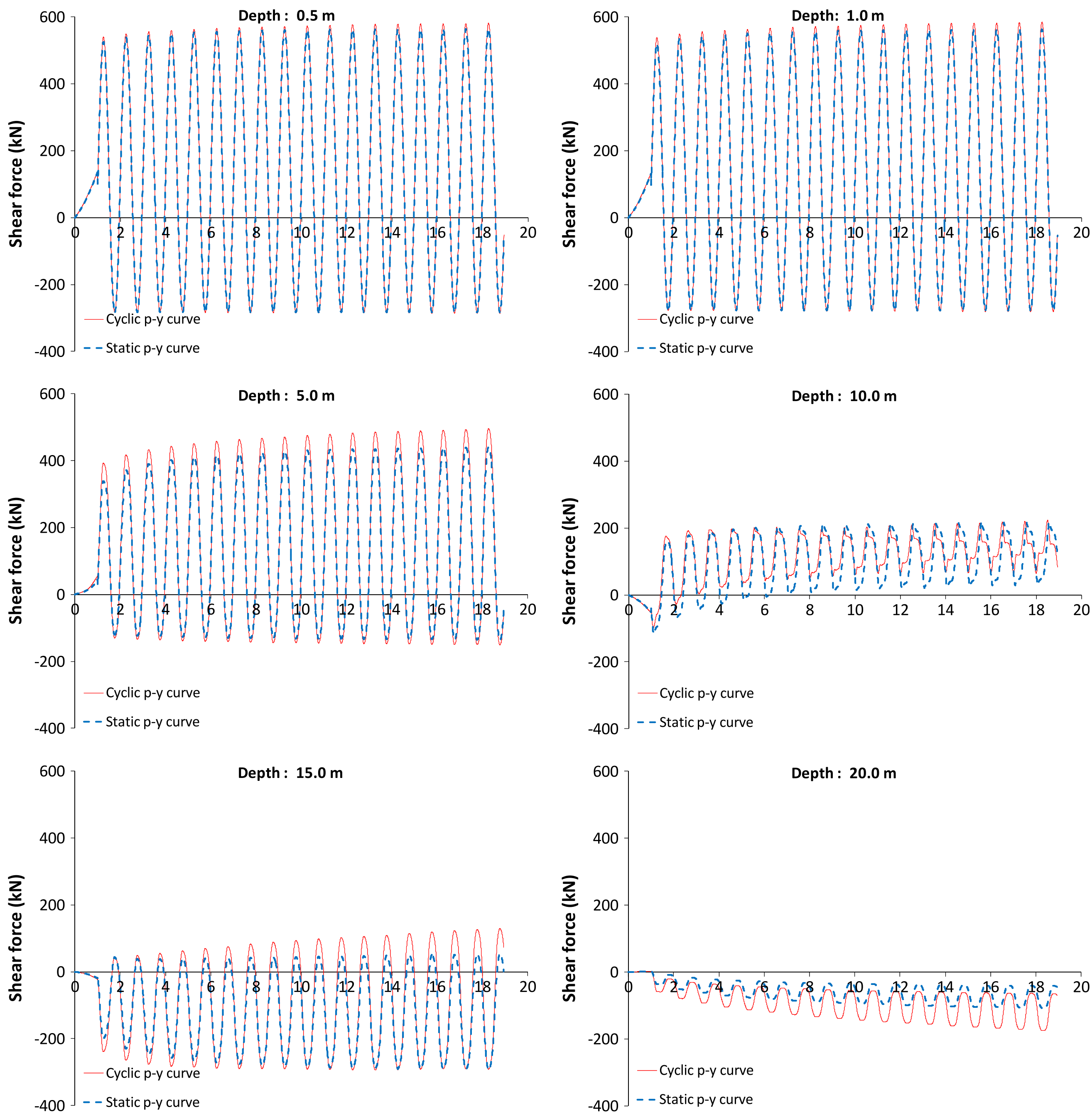

Fig. 15. Pile shear forces at different soil layers.

the elastic range of deflections) will be equal to total applied load on the pile. Soil strength degradation as presented in cyclic *p*–*y* curves (refer to Fig. 3), will result in a larger number of soil layers involved in taking the pile loads. In this case, higher pile internal forces and deeper critical sections are unavoidable.

Lateral deflection time history of the platform (node A of topside in Fig. 9) under cyclic and monotonic loads are compared in Fig. 19. It is seen that under cyclic loads, platform deflections show an initial increasing trend and then after few cycles it continues with a constant harmonic amplitude. Maximum deflection of the platform under cyclic loads and using cyclic *p*–*y* curves is about 13% higher than cyclic loads with static *p*–*y* curves and about 22% higher than monotonic loads with cyclic *p*–*y* curves (which are traditionally used in engineering practice for structural assessment of platforms under wave loads). It can be of great importance for ultimate strength (pushover) analysis of offshore platforms where cyclic behaviour of the structural components and second order loads (P-Delta) effects should also be taken into account.

CPSI model easily allows the user to adjust the amount of the drag force when the pile is moving in the gapped zone. The pile maximum responses for two different drag forces (30% and 60% of the ultimate soil strength) after 10th cycle of the loads using static and cyclic *p*–*y* curves are summarized in Table 3. It is seen that the effect of the drag force ratio is less than 5% and it has no major effect on the response of the maximum response of the piles.

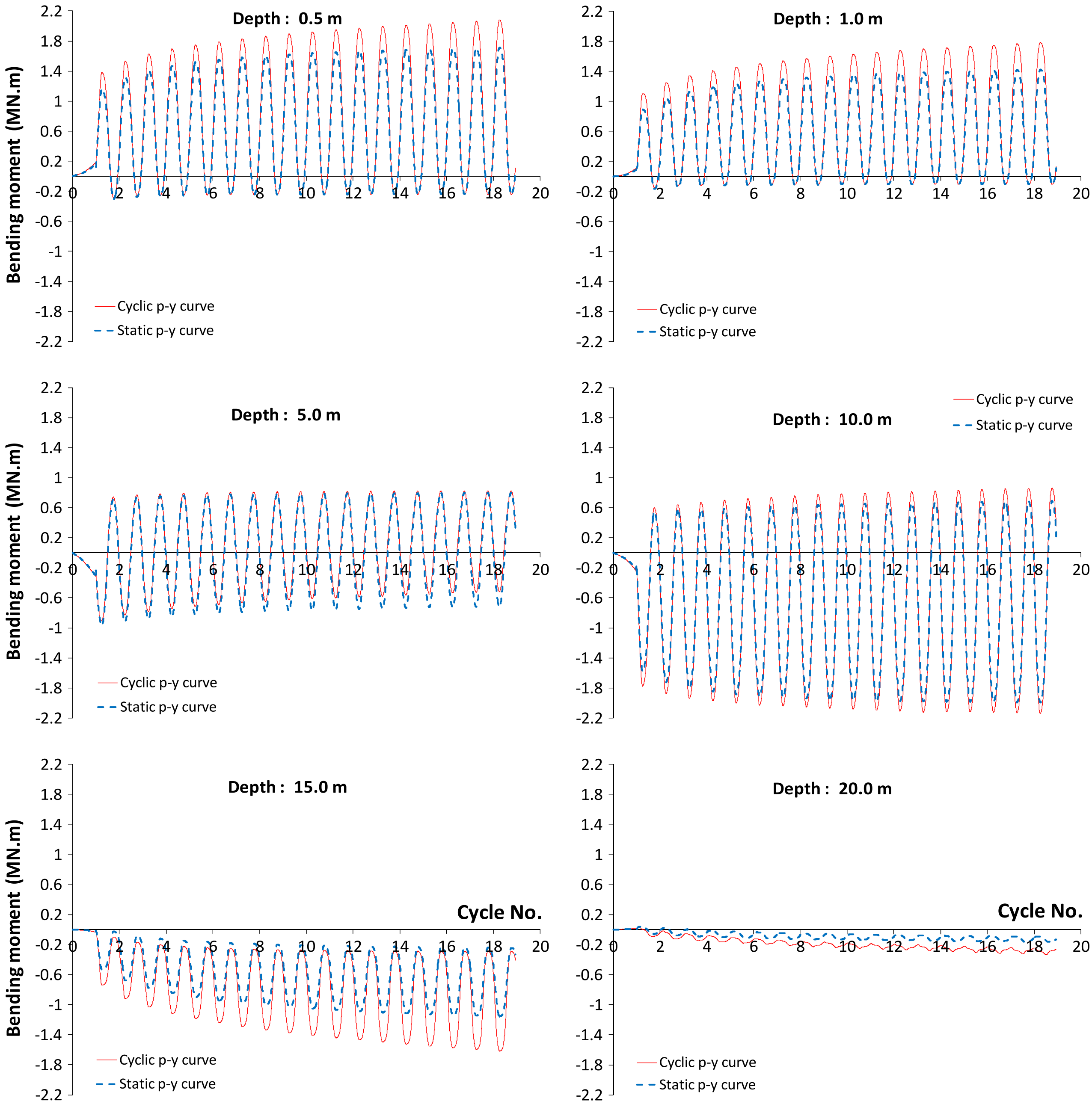

Fig. 16. Pile bending moments at different soil layers.

5. Conclusion

A simplified and robust BNWF model, CPSI, for cyclic pile soil interaction analysis of offshore piles was introduced. This model was incorporated as a user element in the ABAQUS software. It is a versatile and practical element based on the BNWF methodology presented by Boulanger et al. [20]. The CPSI model can take into account the elastic–plastic behaviour of soil layers under cyclic or monotonic loads using API recommended curves for static or cyclic behaviour. Gap formation, gap developments and drag force are the main features of this model for cyclic loads. This model allows the user to easily switch between cyclic and monotonic loads, static and cyclic backbone curves and to adjust the amount of the drag force.

The sensitivity of an example pile supported offshore frame to cyclic and monotonic lateral loads was investigated in this paper. It was found that under cyclic loads the pile's maximum deflections and internal forces increase in the first few cycles and then after higher number of load cycles, asymptotically reach a steady condition with constant amplitudes. It was also shown that the pile responses (deflections, shear forces and bending moments) for cyclic curves were more sensitive to cyclic loads than the pile results using static backbone curves. Gap developments and soil strength degradation transfer the soil resistances from surface soil layers to deeper

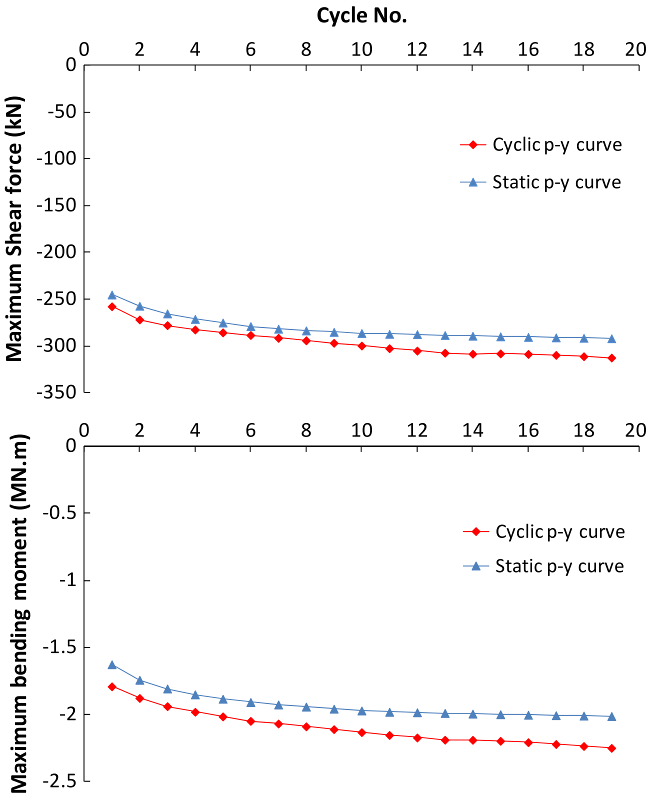

Fig. 17. Pile maximum shear forces and bending moments.

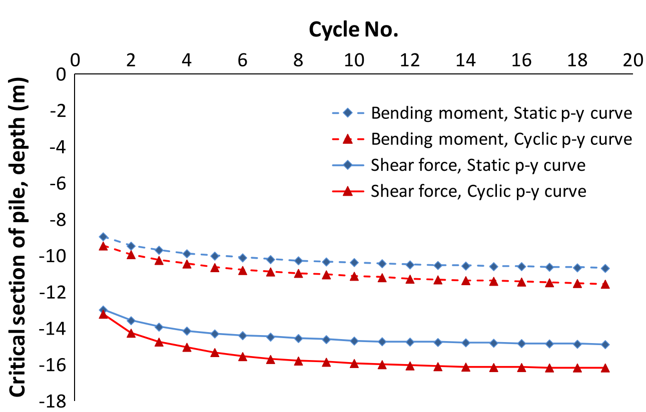

Fig. 18. Pile critical section.

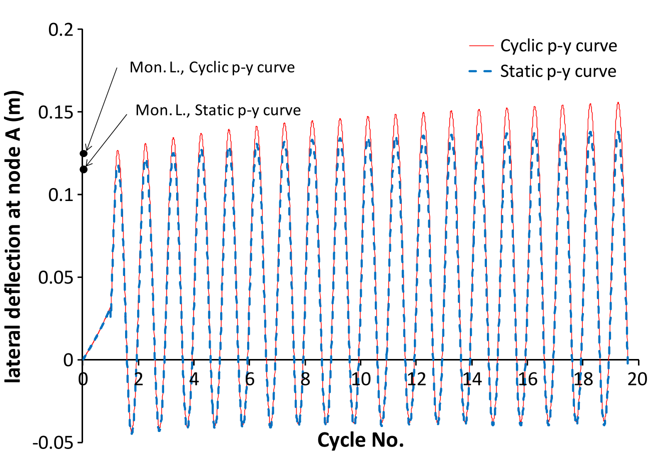

Fig. 19. Platform lateral deflection.

Table 3
Maximum pile responses for different drag forces.

Pile response	*p–y* Curve	30% p_{ult} Drag force	60% p_{ult}	Difference (%)
Deflection (m)	Static	0.166	0.161	2.75
	Cyclic	0.200	0.191	4.7
Shear force (kN)	Static	287	280	2.4
	Cyclic	302	290	3.9
Bending moment (MN m)	Static	1.98	1.94	2.3
	Cyclic	2.15	2.07	3.6

soil layers which finally lead to increased pile response and the moving of the critical section of the piles downward along the pile shaft.

Lateral cyclic deflection of the platform using cyclic backbone curves is considerably higher than the corresponding results under monotonic loads. It can have significant effects on ultimate capacity of the platforms where cyclic behaviour of the platform and second order effects (P-Delta) are of importance.

Acknowledgment

The authors would like to thank COFS (Centre for Offshore Foundation Systems) at UWA (University of Western Australia) and IUST (Iran University of Science and Technology) for their technical and financial supports during this study.

References

[1] Bea RG. Earthquake geotechnology in offshore structures. In: 2nd International conference on recent advances in geotechnical earthquake engineering and soil dynamics. St. Louis, Missouri; 1991. p. 9–22.
[2] Gerolymos N, Escoffi S, Gazetas G, Garnier J. Numerical modeling of centrifuge cyclic lateral pile load experiments. Earthquake Eng Eng Vib 2009;8(1):61–76.
[3] Broms BB. Lateral resistance of piles in cohesive soils. J Soil Mech Found Div ASCE 1964;90(2):27–63.
[4] Yegian M, Wright S. Lateral soil resistance–displacement relationships for pile foundations in soft clays. In: 5th Offshore technology conference. Texas, Houston; 1973. p. 663–76.
[5] Randolph M. Response of flexible piles to lateral loading. Géotechnique 1981;31(2):247–59.
[6] Trochanis A, Bielak J, Christiano P. A three dimensional nonlinear study of piles leading to the development of a simplified model. Report R-88-176. Pittsburgh: Department of Civil Engineering, Carnegie Institute of Technology; 1988.
[7] Bentley KJ, El Naggar MH. Dynamic analysis for laterally loaded piles and dynamic *p–y* curves. Can Geotech J 2000;37(6):1166–83.
[8] Kaynia A, Kausel E. Dynamic stiffness and seismic response of pile groups. Report R82-03. Cambridge, Mass: Massachusetts Institute of Technology; 1982.
[9] Sen R, Davis TG, Banerjee PK. Dynamic analysis of piles and pile groups embedded in homogenous soils. Int J Earthquake Eng Struct Dyn 1985;13(1):53–65.
[10] Millán MA, Domínguez J. Simplified BEM/FEM model for dynamic analysis of structures on piles and pile groups in viscoelastic and poroelastic soils. Eng Anal Bound Elem 2009;33(1):25–34.
[11] Padrón LA, Aznárez JJ, Maeso O. BEM–FEM coupling model for the dynamic analysis of piles and pile groups. Eng Anal Bound Elem 2007;31(6):473–84.
[12] Matlock H, Foo HC, Brayant LM. Simulation of lateral pile behavior under earthquake motion. In: American society of civil engineers specialty conference on earthquake engineering and soil dynamics. Pasadena, California; 1978. p. 600–19.
[13] Makris M, Gazetas G. Dynamic pile–soil–pile interaction. Part II: lateral and seismic response. Earthquake Eng Struct Dyn 1992;21(2):145–62.
[14] Nogami T, Konagai K, Otani J, Chen HL. Nonlinear soil–pile interaction model for dynamic lateral motion. J Geotech Eng ASCE 1992;118(1):106–16.
[15] El Naggar MH, Novak M. Nonlinear lateral interaction in pile dynamics. Soil Dyn Earthquake Eng 1995;14(2):141–57.
[16] El Naggar MH, Novak M. Nonlinear analysis for dynamic lateral pile response. Soil Dyn Earthquake Eng 1996;15(4):233–44.
[17] Trochanis A, Bielak J, Christiano P. Simplified model for analysis of one or two piles. J Geotech Eng ASCE 1991;117(3):448–66.
[18] Badoni D, Makris N. Nonlinear response of single piles under lateral inertial and seismic loads. Soil Dyn Earthquake Eng 1995;15(1):29–43.
[19] Wang S, Kutter BL, Chacko MJ, Wilson DW, Boulanger RW, Abghari A. Nonlinear seismic soil–pile structure interaction. Earthquake Spectra 1998;14(2):377–96.

[20] Boulanger RW, Curras CJ, Kutter BL, Wilson DW, Abghari A. Seismic soil–pile–structure interaction experiments and analysis. J Geotech Geoenviron Eng ASCE 1999;125(9):750–9.
[21] Kimiaei M, Shayanfar MA, El Naggar MH, Aghakoochak AA. Non linear seismic pile soil structure interaction analysis of piles in offshore platforms. In: 23rd International conference on offshore mechanics and arctic engineering. Vancouver; 2004. p. OMAE2004-51006.
[22] Wotherspoon LM, Sritharan S, Pender MJ. Modelling the response of cyclically loaded bridge columns embedded in warm and seasonally frozen soils. Eng Struct 2010;32(4):933–43.
[23] Konuk I, Fredj A. FEM model for pipeline analysis of ice scour – a critical review. In: 23rd International conference on offshore mechanics and arctic engineering. Vancouver, Canada; 2004.
[24] Fredj A, Comfort G, Dinovitzer A. A case study of high pressure/high temperature pipeline for ice scour design using 3D continuum modeling. In: 27th International conference on offshore mechanics and arctic engineering. Estoril, Portugal; 2008.
[25] Blum H. Einspannungsverhaltnisse bei Bohlwerken. Berlin: Wilhelm Ernst & Sohn; 1931.
[26] Norris GM. Theoretically based BEF laterally loaded pile analysis. In: 3th International conference on numerical methods in offshore piling. Nantes, France; 1986. p. 361–86.
[27] Ashour M, Norris G. Modeling lateral soil–pile response based on soil–pile interaction. J Geotech Geoenviron Eng ASCE 2000;126(5):420–8.
[28] Matlock H. Correlations for design of laterally loaded piles in soft clay. In: 2nd Offshore technology conference. Houston, Texas; 1970. p. 577–88.
[29] Reese L, Welch R. Lateral loading of deep foundations in stiff clay. J Geotech Eng ASCE 1975;101(7):633–49.
[30] Reese LC, Cox WR, Koop FD. Analysis of Laterally Loaded in Sand. In: 6th Offshore technology conference. Houston, Texas; 1974. p. 473–83.
[31] Recommended practice for planning, designing, and constructing fixed offshore platforms – working stress design. Report RP 2A-WSD. Dallas: American Petroleum Institute; 2000.
[32] ABAQUS. 6.5.1 ed: Simulia Inc.; 2004.
[33] Memarpour MM, Kimiaei M, Shayanfar MA. A new BNWF model for cyclic pile–soil interaction analysis of single offshore piles. In: 13th International conference of the international association for computer methods and advances in geomechanics melbourne. Australia; 2011. p. 135–40.
[34] Memarpour MM, Kimiaei M, Shayanfar MA. Simplified numerical model for analysis of offshore piles under cyclic lateral loading. In: 2nd International symposium on frontiers in offshore geotechnics. Perth, Australia; 2010. p. 531–6.
[35] Mazzoni S, McKenna F, Scott M, Fenves G. OpenSees command language manual. 2007. <http://opensees.berkeley.edu>.
[36] Wallace JW, Fox PJ, Stewart JP, Janoyan K, Qiu T, Lermitte SP. Cyclic large deflection testing of shaft bridges. Part II: Analytical studies. Los Angeles. Department of Civil and Environmental Engineering University of California; 2002.
[37] Grabe J, Mahutka KL, Dührkop J. Monopilegründungen von Offshore–Windenergieanlagen – Zum Ansatz der Bettung. Bautechnik 2005;82(1):1–10.